Molecular Therapy
Nucleic Acids
Original Article

circPHIP promotes oral squamous cell carcinoma progression by sponging miR-142-5p and regulating PHIP and ACTN4 expression

Wen Su,[1,2,3,4,5] Yuehong Shen,[1,2,3,5] Yufan Wang,[1,2,3] Feng Wang,[1,2,3] Xia Hong,[1,2,3] Yuling Chen,[1,2,3] Yuntao Lin,[1,2,3] and Hongyu Yang[1,2,3]

[1]Department of Oral and Maxillofacial Surgery, Stomatological Center, Peking University Shenzhen Hospital, Shenzhen, Guangdong, China; [2]Guangdong Provincial High-Level Clinical Key Specialty, Guangzhou, China; [3]Guangdong Province Engineering Research Center of Oral Disease Diagnosis and Treatment, Guangzhou, China; [4]State Key Laboratory Breeding Base of Basic Science of Stomatology (Hubei-MOST), Key Laboratory of Oral Biomedicine Ministry of Education, School and Hospital of Stomatology, Wuhan University, 430079 Wuhan, China

Circular RNA (circRNA) is a newly discovered class of noncoding RNAs that plays key regulatory role in pathological development, including the regulation of several solid tumors. However, the effects of circRNA expression on oral squamous cell carcinoma (OSCC) remain unclear. With the use of high-throughput RNA sequencing data on eight paired oral cancer and adjacent healthy tissues, we observed that circRNA derived from the gene encoding pleckstrin homology domain-interacting protein (circPHIP) was highly expressed in OSCC. Additionally, circPHIP was highly expressed in other OSCC-related cell lines and was associated with tumor metastasis, TNM stage, and human papilloma virus infection status. The inhibition of circPHIP expression reduced OSCC cell migration, invasion, and proliferation. We found that circPHIP could adsorb microRNA (miR)-142-5p and upregulate the expression of PHIP and alpha-actinin 4 (ACTN4), both of which are potential oncogenes closely related to OSCC prognosis. The inhibition of miR-142-5p or overexpressing PHIP or ACTN4 reversed the circPHIP depletion-induced attenuation of OSCC malignancy. In conclusion, circPHIP is overexpressed in OSCC and enhances its malignancy via an miR-142-5p/PHIP-ACTN4/AKT serine/threonine kinase 1 signaling axis. Therefore, circPHIP may represent a novel target for treating OSCC.

INTRODUCTION

Oral squamous cell carcinoma (OSCC) is the most common head and neck malignancy. It presents with different degrees of differentiation and is prone to lymph node metastasis, resulting in poor prognosis.[1,2] The treatment involves surgery in combination with radiotherapy and chemotherapy; however, most patients experience recurrence or distant metastasis, and its 5-year survival rate is ~60%.[3–5] The improvement of OSCC survival rates is a difficult public health issue, and new therapies are urgently needed, especially targeted therapies affecting complex gene-regulatory networks.

Circular RNAs (circRNAs) are noncoding RNA molecules. They are closed circular structures lacking a 5′ cap and a 3′ polyadenylated tail; this absence of the 5′ cap and 3′ polyadenylated tail confers their unique functions.[6,7] circRNAs are evolutionarily conserved, stable, abundant, and specifically expressed in different cells and developmental stages.[8] Functions of circRNAs include sponging microRNAs (miRNAs), interacting with RNA-binding proteins, and participating in protein translation.[9–12] circRNAs are involved in regulating malignant tumors; thus, specific circRNAs are expected to be adopted as tumor biomarkers.[13–16]

miRNAs are noncoding single-stranded RNA molecules comprising 20–24 nucleotides and are encoded by endogenous genes.[17] miRNAs can combine with specific target mRNAs to degrade them, inhibiting their normal translation process, thereby regulating gene expression in the post-transcription stage, and widely participating in cellular processes, such as growth, development, differentiation, metabolism, and immune response.[18] The differentially expressed miRNAs between normal and tumor cells function similarly as proto-oncogenes or tumor-suppressor genes by regulating different target genes and are thus involved in cancer development, tumorigenesis, and prognosis.[19–21]

There is an intricate interaction between coding and noncoding RNAs. The two RNA transcripts are used as competitive endogenous RNAs (ceRNAs), i.e., miRNA sponges, to precisely regulate signaling networks by competing against shared miRNAs and thus significantly impact tumorigenesis and development.[22] Previous studies have identified thousands of circRNAs in the mammalian transcriptome, suggesting that circRNAs may represent a new class of ceRNA

Received 5 August 2020; accepted 29 October 2020;
https://doi.org/10.1016/j.omtn.2020.10.038.

[5]These authors contributed equally

Correspondence: Yuehong Shen, Department of Oral and Maxillofacial Surgery, Peking University Shenzhen Hospital, Shenzhen, Guangdong, China.
E-mail: yuehongshen@hotmail.com
Correspondence: Hongyu Yang, Department of Oral and Maxillofacial Surgery, Peking University Shenzhen Hospital, Shenzhen, Guangdong, China.
E-mail: hyyang192@hotmail.com

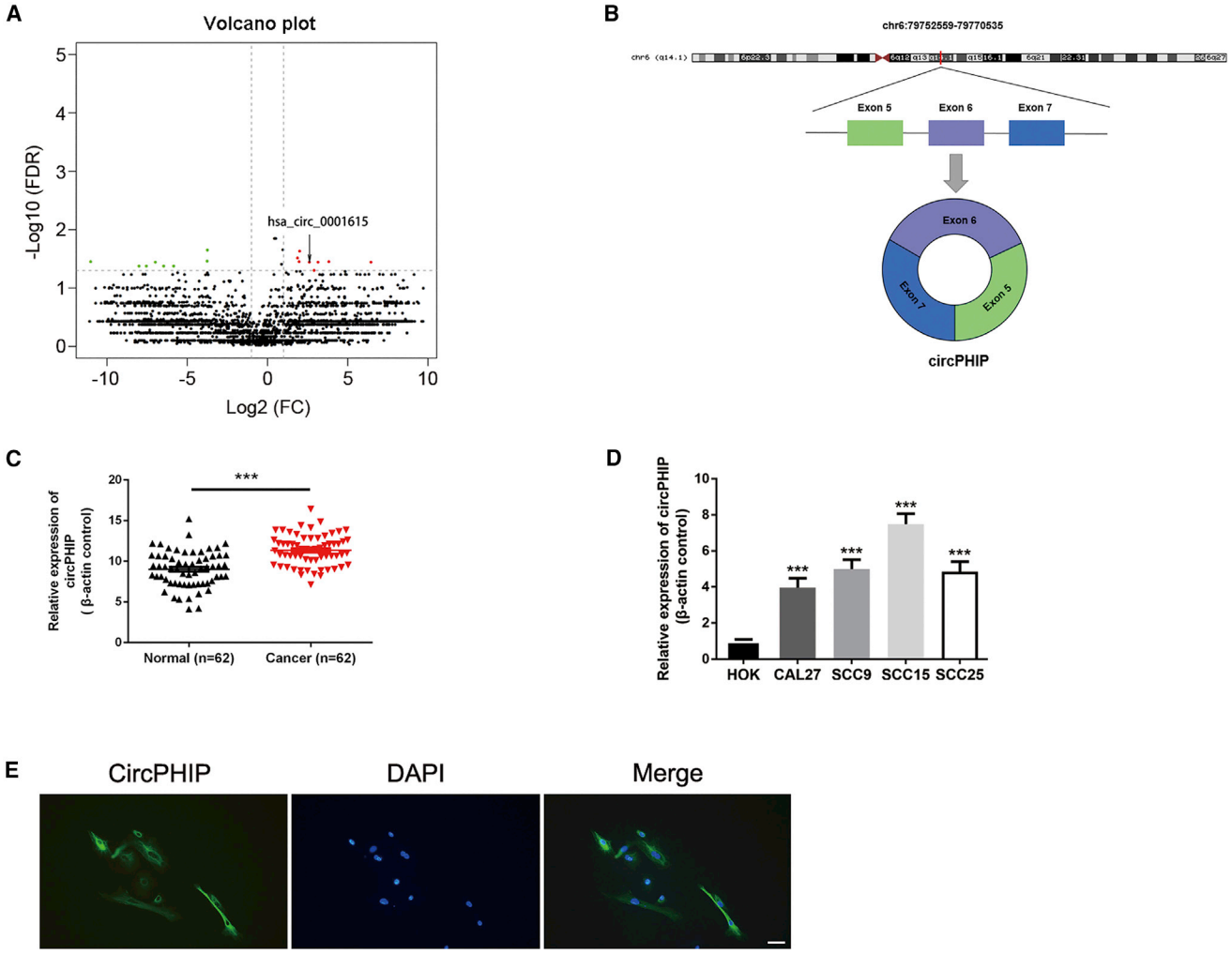

Figure 1. Identification and validation of differential circPHIP expression in OSCC tissues and cells

(A) Volcano plot of differentially expressed circRNAs. The green dots are downregulated circRNAs, whereas the red dots are upregulated circRNAs in OSCC. circPHIP is labeled as hsa_circ_0001615. (B) Schematic showing the circularization of *PHIP* exons 5–7 forming circPHIP. (C) circPHIP expression was detected via qRT-PCR in 62 pairs of OSCC and adjacent normal tissues. Student's t test, ***$p < 0.001$. (D) circPHIP expression was detected via qRT-PCR in various human OSCC cell lines (CAL27, SCC15, SCC9, and SCC25) and healthy oral keratinocytes (HOKs). (E) FISH analysis of circPHIP localization. Scale bar, 50 μm.

regulators.[16,23] Owing to their high expression levels and increased stability, circRNAs with ceRNA activity may effectively modulate the crosstalk between linear ceRNAs.[24] Recent studies have found that circRNA CDR1 (ciRS-7) is highly stable and contains more than 60 conserved binding sites for microRNA (miR)-7 and can effectively sponge miR-7 and affect its targeting activity.[25,26] The analysis of ceRNA crosstalk may provide insights into the function of various circRNAs.

OSCC development and progression are regulated by various coding and noncoding genes; however, the role of circRNAs in these processes is unclear.[27] In this study, we characterized a circRNA derived from the gene encoding pleckstrin homology domain-interacting protein (*PHIP*), circPHIP (hsa_circ_0001615). circPHIP was upregulated in OSCC tissues and cell lines and associated with OSCC metastasis, TNM stage, and human papilloma virus (HPV) infection status. Herein, we propose that circPHIP regulates PHIP and alpha-actinin 4 (ACTN4) expression by adsorbing miR-142-5p, thereby affecting OSCC progression and metastasis.

RESULTS

circPHIP (hsa_circ_0001615) is highly expressed in OSCC

Previously, we screened for differentially expressed circRNAs by analyzing eight pairs of OSCC and healthy oral mucosal tissues through high-throughput RNA sequencing.[28] From a volcano map of the results, we identified the significantly overexpressed circRNA circPHIP, which is transcribed from *PHIP* on human chromosome 6 by head-to-tail splicing of exons 5–7 (Figures 1A and 1B). To

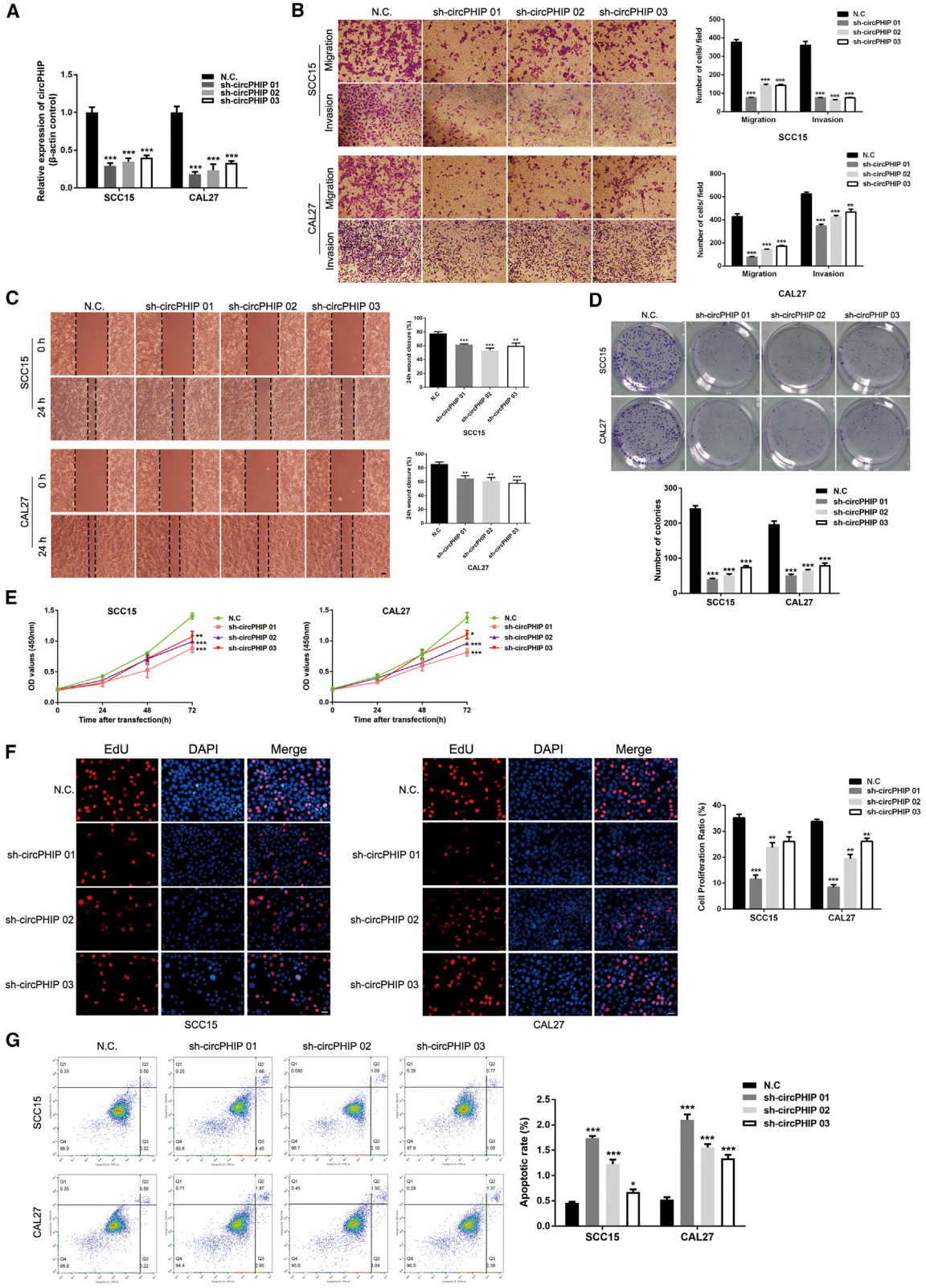

(legend on next page)

examine the correlation between circPHIP expression and OSCC, we collected 62 pairs of healthy and oral cancer tissue samples and used quantitative reverse-transcriptase polymerase chain reaction (qRT-PCR) to detect circPHIP expression. The expression of circPHIP was higher in OSCC tissues than in healthy oral tissues (Figure 1C), consistent with the RNA sequencing results. We next examined circPHIP expression in OSCC cell lines. Compared to its level in healthy oral keratinocytes (HOKs), circPHIP levels significantly increased in all four OSCC cell lines (CAL27, SCC9, SCC15, and SCC25), particularly in SCC15 cells (Figure 1D). Therefore, we conducted RNA fluorescence *in situ* hybridization (FISH) experiments in SCC15 cells and observed that circPHIP was mainly localized to the cytoplasm (Figure 1E). Additionally, we analyzed the relationships between circPHIP expression levels and clinical parameters of OSCC (Table S1). The circPHIP expression level was related to lymph node metastasis, clinical stage, and HPV infection status, confirming the clinical value of studying this circRNA.

Depleting circPHIP inhibits OSCC cell migration, invasion, and proliferation

To explore the mechanism by which circPHIP regulates OSCC, we used short hairpin RNAs (shRNAs) to reduce circPHIP expression. We designed three shRNAs and transfected them into SCC15 and CAL27 cells. Transfection efficiency assessment via qRT-PCR demonstrated significant depletion of circPHIP (Figure 2A). The depletion significantly reduced the migration and invasion of SCC15 and CAL27 cells (Figures 2B and 2C). Knocking down circPHIP significantly inhibited the colony-forming ability of OSCC cells (Figure 2D), indicating decreased proliferation. This observation was also verified using Cell Counting Kit-8 (CCK-8) (Figure 2E) and 5-ethynyl-2′-deoxyuridine incorporation (EdU) (Figure 2F) assays. Additionally, the depletion of circPHIP inhibited apoptosis of OSCC cells (Figure 2G). Of the three shRNAs, sh-circPHIP 01 had the highest knockdown efficiency and was used in subsequent experiments. Taken together, these findings reveal that circPHIP plays important roles in OSCC cells.

circPHIP functions as an efficient sponge for miR-142-5p in OSCC

To investigate whether circPHIP can function as an miRNA sponge, we transfected HOKs with the Argonaute RNA-induced silencing complex (RISC) catalytic component 2 (AGO2) plasmid and conducted RNA immunoprecipitation (RIP) analysis. Endogenous circPHIP was specifically enriched in the AGO2 overexpression group (Figure 3A). Four databases were used to predict potential target miRNAs: miRTarBase, http://mirtarbase.mbc.nctu.edu.tw/php/index.php/; miRDB, http://www.mirdb.org/; mirDIP, http://ophid.utoronto.ca/mirDIP/; and TargetScanHuman, http://www.targetscan.org/vert_70/ (Figure 3B). The miRNA miR-142-5p was selected for further investigation. To confirm the predicted interaction, we performed pulldown assays with a biotinylated circPHIP probe. In both SCC15 and CAL27 cells, miR-142-5p was significantly enhanced upon circPHIP capture (∼2-fold increase in SCC15 cells and ∼4-fold increase in CAL27 cells; Figure 3C). These results were orthogonally validated using luciferase assays. Bioinformatics analysis using CircInteractome (https://circinteractome.nia.nih.gov/) revealed a shared miRNA response element (MRE) between circPHIP and miR-142-5p. Therefore, we mutated this MRE (mutant [Mut]) and cloned it into the luciferase reporter gene in place of the wild-type (WT) circPHIP 3′ untranslated regions (UTRs) (Figure 3D). After transfecting miR-142-5p into HOKs, the luciferase activity of the Mut reporter was significantly higher than that of the WT reporter (Figure 3E), indicating that miR-142-5p could directly bind to circPHIP.

miR-142-5p is downregulated in OSCC cells and tissues and inhibits OSCC malignancy

We used qRT-PCR to detect miR-142-5p expression in OSCC tissues (Figure 4A) and cell lines (Figure 4B). Compared with healthy oral mucosa samples, miR-142-5p expression was significantly reduced in OSCC tissue samples. Kaplan-Meier analysis using the Kaplan-Meier Plotter (http://kmplot.com/analysis/) revealed that miR-142-5p was significantly associated with the overall survival of patients with head and neck cancer (Figure 4C), with worse prognosis at decreased miR-142-5p levels. As miR-142-5p expression was significantly reduced in OSCC tissues, we next analyzed whether it was related to the clinicopathological stage of patients with OSCC. FISH analysis of 62 tissue pairs revealed that miR-142-5p expression was negatively correlated with the clinical pathological stage of OSCC. From stages I to IV, miR-142-5p expression showed a significant downward trend (Figure 4D). Furthermore, we used miR-142-5p inhibitors or mimics to inhibit or promote miR-142-5p expression, respectively. Transwell migration and invasion and wound-healing assays revealed that miR-142-5p overexpression inhibited OSCC cell migration and invasion (Figures 4E and 4F). In colony-formation and CCK-8 assays, miR-142-5p downregulation significantly promoted cell viability (Figures 4G and 4H). Moreover, flow cytometry analysis showed that miR-142-5p downregulation inhibited OSCC cell apoptosis (Figure 4I). Overall, these results indicate that miR-142-5p inhibits the migration, invasion, and proliferation of OSCC cells *in vitro*.

Figure 2. circPHIP inhibits the migration, invasion, and proliferation of OSCC

(A) After stable transfection of sh-circPHIP or negative control (NC) vector, circPHIP expression levels in SCC15 and CAL27 cells were detected using qRT-PCR. (B) Transwell migration and invasion assays in stable SCC15 and CAL27 cells with circPHIP knockdown. (C) Wound-healing assays in stable SCC15 and CAL27 cells with circPHIP knockdown. (D) Colony-formation assays in stable SCC15 and CAL27 cells with circPHIP knockdown. (E) CCK-8 assays were performed in stable SCC15 and CAL27 cells with circPHIP knockdown. (F) EdU incorporation assays in stable SCC15 and CAL27 cells with circPHIP knockdown. (G) Annexin V-fluorescein isothiocyanate (FITC)/propidium iodide (PI) staining of stable SCC15 and CAL27 cells with circPHIP knockdown. The percentage of apoptotic cells is shown. All data are presented as mean ± SEM of three independent experiments. Student's t test, *$p < 0.05$, **$p < 0.01$, ***$p < 0.001$. Representative images are shown. Scale bars, 20 μm.

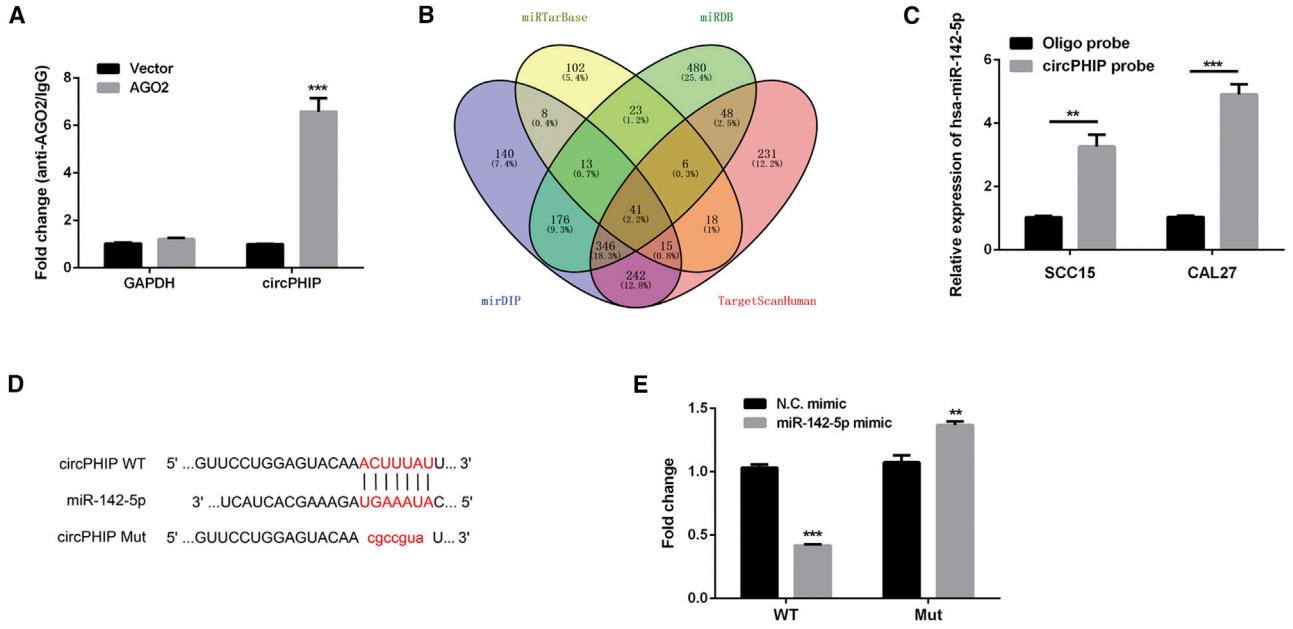

Figure 3. circPHIP acts as an miR-142-5p sponge in OSCC cells

(A) RIP assay was performed to detect circPHIP levels in HOKs transfected with AGO2. (B) Schematic exhibiting the overlap in circPHIP target miRNAs predicted by the miRTarBase, miRDB, mirDIP, and TargetScanHuman databases. (C) Relative miR-142-5p levels in SCC15 and CAL27 lysates. (D) Predicted circPHIP and miR-142-5p binding sites. (E) Luciferase activities of HOKs cotransfected with a luciferase reporter construct containing wild-type (WT) or mutant (Mut) circPHIP and miR-142-5p or NC mimic. All data are presented as mean ± SEM of three independent experiments. Student's t test, $^{**}p < 0.01$, $^{***}p < 0.001$.

Silencing miR-142-5p reverses the antitumor effects of circPHIP depletion in OSCC cells

We next designed rescue experiments to explore whether circPHIP enhances the malignant behavior of OSCC by interacting with miR-142-5p. SCC15 and CAL27 cells were stably cotransfected with the sh-circPHIP lentiviral vector and miR-142-5p inhibitor. Transwell migration and invasion and wound-healing assays demonstrated that miR-142-5p sponging partially reversed the inhibited migration and invasion caused by circPHIP depletion (Figures 5A and 5B). In addition, the inhibitory effect on miR-142-5p partially attenuated the reduced viability induced via sh-circPHIP, as demonstrated by CCK-8 and colony-formation assays (Figures 5C and 5D). Flow cytometry analysis showed that the proportion of apoptotic cells significantly decreased after sh-circPHIP/miR-142-5p inhibitor cotreatment (Figure 5E). These findings indicate that circPHIP promotes OSCC progression by eliminating the antitumor effects of miR-142-5p.

PHIP and *ACTN4* are direct targets of miR-142-5p and are oncogenic in OSCC

To confirm whether *PHIP* and *ACTN4* are potential miR-142-5p target genes, we generated 3′ UTR sensors into the downstream of the luciferase reporter and cotransfected them into HOKs with miR-142-5p mimics. When miR-142-5p was overexpressed, both *PHIP* and *ACTN4* showed a reduced luciferase activity. Conversely, when the Mut forms of the *PHIP* and *ACTN4* (with the miR-142-5p binding site disrupted) were used, we observed much higher luciferase activity (Figures 6A and 6B). Interestingly, the mRNA expression of *PHIP* and *ACTN4* in OSCC tissues and cell lines was higher than that in healthy mucosal tissues and cells (Figures 6C and 6D). The transcript levels of *PHIP* and *ACTN4* were significantly reduced when SCC15 and CAL27 cells were transfected with sh-circPHIP (Figure 6E). Gene Expression Profiling Interactive Analysis (http://gepia.cancer-pku.cn/) revealed a coexpression relationship between *PHIP* and *ACTN4* (Figure S1). With the use of OSCC cells with stable miR-142-5p knockdown or overexpression, we performed immunoblotting for the following proteins: B cell lymphoma-2 (Bcl-2), a critical indicator of cell proliferation and apoptosis;[29] matrix metallopeptidase 9 (MMP9), a tumor invasion- and metastasis-promoting factor;[30] AKT phosphorylated (p)-AKT; mechanistic target of rapamycin kinase (mTOR); and p-mTOR, members of the phosphatidylinositol 3-kinase (PI3K)/AKT/mTOR pathway that regulates cell growth, protein translation, survival, and metabolism.[31] The results showed that the levels of PHIP, ACTN4, Bcl-2, MMP9, AKT, p-AKT, mTOR, and p-mTOR were inversely related to miR-142-5p expression (Figures 6F and 6G). Together, these results indicate that a PHIP-ACTN4/AKT/mTOR signaling axis is regulated via circPHIP by sponging miR-142-5p in OSCC.

circPHIP promotes OSCC progression via PHIP and ACTN4

To further explore whether circPHIP affects OSCC malignancy by regulating PHIP and ACTN4, we used bioinformatics analysis to investigate the roles of PHIP and ACTN4 in tumor progression. We probed database: The Cancer Genome Atlas (TCGA) and revealed that patients with head and neck tumors that overexpress *ACTN4* and *PHIP* have a poor

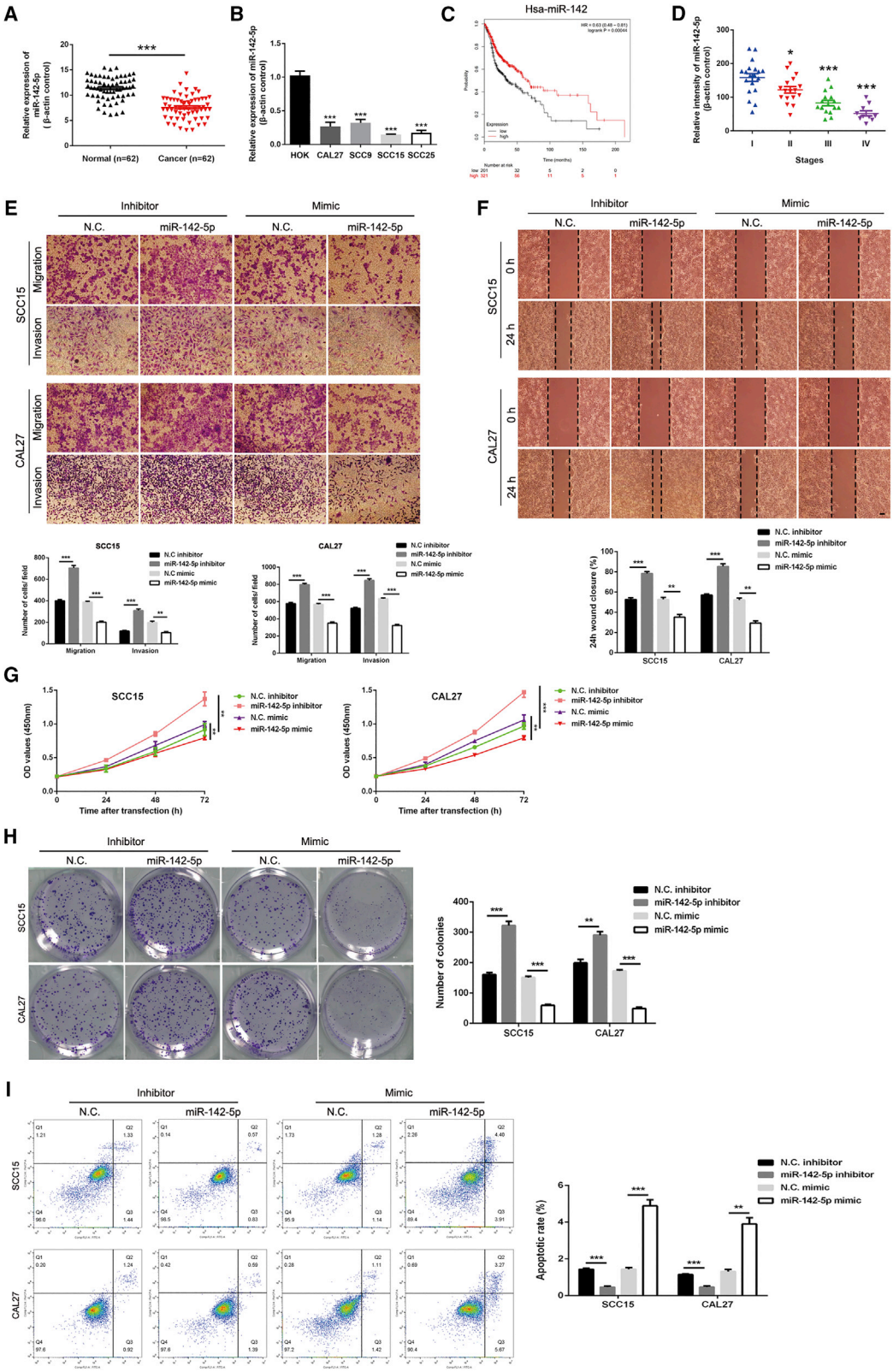

(legend on next page)

prognosis (Figure S2A). Compared with HPV-negative patients, the expression of *ACTN4* and *PHIP* was higher in HPV-positive patients (Figure S2B). These results indicate that the expression of *PHIP* and *ACTN4* correlated with survival and HPV infection status in patients with head and neck tumors. Thus, we set out a series of experiments to study how circPHIP regulates PHIP and ACTN4 in OSCC cells. Lentiviral overexpression vectors were constructed and transfected into circPHIP-depleted SCC15 and CAL27 cells. PHIP and ACTN4 overexpression partially reversed the decreased Bcl-2, MMP9, p-AKT, and p-mTOR levels induced via circPHIP knockdown (Figure 7A). We then explored whether PHIP and ACTN4 improved the metastatic capacity of tumor cells. Compared with cells treated with sh-circPHIP alone, cells overexpressing PHIP and ACTN4 had significantly improved migration and invasion capabilities (Figures 7B and 7C). In addition, CCK-8 assays demonstrated that PHIP and ACTN4 expression improved the viability of OSCC cells (Figure 7D). The colony-forming ability of the tumor cells significantly increased (Figure 7E). PHIP and ACTN4 expression also inhibited apoptosis, as demonstrated via flow cytometry (Figure 7F). These findings indicate that circPHIP promotes OSCC malignancy by regulating PHIP and ACTN4.

circPHIP enhances the growth and metastasis of tumor xenografts *in vivo*

To examine the functions of circPHIP and miR-142-5p *in vivo*, we established a tumor xenograft model. Stable SCC15 cells expressing the negative control (NC) or sh-circPHIP, with or without the miR-142-5p inhibitor, were subcutaneously injected into nude mice. The sizes and weights of tumors derived from the circPHIP-depleted cells were reduced compared to those from the control group. Interestingly, miR-142-5p inhibition significantly reversed the decreased tumor size and weight after circPHIP silencing (Figures 8A–8C). Consistently, immunoblotting results of proteins extracted from the tumors showed a decrease in PHIP, ACTN4, Bcl-2, MMP9, p-AKT, and p-mTOR levels after circPHIP depletion, whereas miR-142-5p inhibition reversed these changes (Figure 8D). Immunohistochemical (IHC) staining confirmed these results (Figure 8E).

DISCUSSION

In recent years, noncoding RNAs have become a research hotspot in the quest to elucidate the mechanisms behind tumorigenesis and cancer progression. circRNAs are a newly discovered class of noncoding RNAs that regulate gene expression and are closely related to many types of tumors, including colon, gastric, and esophageal cancers.[14,16,32] Differential circRNA expression is significantly associated with distant metastasis, TNM stage, and other clinical features of cancer.[33] Therefore, circRNAs provide new directions for studying tumor pathogenesis and potential biomarkers for a variety of cancers.

ceRNAs regulate gene expression and are postulated to act via MREs to form a large-scale transcriptional regulatory network in which mRNAs, pseudogenes, long-chain noncoding RNAs, and circRNAs can "interact" with each other, potentially affecting certain pathological conditions.[26,34,35] Many studies have shown that ceRNAs play important roles in the expansion, invasion, and metastasis of tumor cells.[36,37] As a novel form of noncoding RNA, circRNAs are also involved in regulating tumor ceRNA networks.[25]

Like other malignant tumors, the development and progression of OSCC include a series of complex biological processes involving both coding and noncoding genes. Therefore, the identification of clinically relevant OSCC-specific circRNAs and the examination of their function and regulatory effects on OSCC are crucial to understanding the disease. By regulating components of key signaling pathways, circRNAs can regulate the malignancy of tumor cells. Understanding these regulatory events will aid the design of more effective anticancer therapies for OSCC, thereby improving patient survival.

In the first stage of this study, we compared circRNA expression levels in OSCC and healthy oral mucosa tissues using high-throughput, next-generation RNA sequencing technology and identified circPHIP. Further research revealed that circPHIP acts as a ceRNA, regulating OSCC cells by adsorbing miR-142-5p, which not only displayed strong binding to circPHIP in both SCC15 and CAL27 cells but also played a key role in OSCC progression and metastasis.

In this study, both *in vivo* and *in vitro* experiments indicated that *PHIP* and *ACTN4* are driver genes in OSCC development. *PHIP* is located on chromosome 6 and encodes a protein involved in the insulin-like growth factor receptor 1/PI3K signaling pathway.[38] Gene-expression profiling identified *PHIP* as overexpressed in metastatic melanoma.[39] Studies on melanoma demonstrated that PHIP is both a marker and regulator of distant metastasis, establishing the idea of targeting PHIP in its treatment.[40] Subsequent research found that PHIP also promotes the progression of breast and lung cancers. The inhibition of PHIP expression can significantly reduce tumor cell proliferation and invasion and synergistically decreases p-AKT and cyclin D1 levels. Therefore, PHIP may be a potential therapeutic target for these tumors as well.[41,42] Our research indicates that *PHIP* acts as an oncogene in

Figure 4. miR-142-5p regulates the migration, invasion, and proliferation of OSCC cells

(A) miR-142-5p expression was detected via qRT-PCR in 62 pairs of OSCC and healthy tissues. (B) miR-142-5p expression was detected via qRT-PCR in human OSCC (CAL27, SCC9, SCC15, and SCC25) and HOKs. (C) Kaplan-Meier analysis of the effects of miR-142-5p expression on the overall survival of patients with head and neck cancer. (D) miR-142-5p expression in different clinicopathological stages of OSCC was analyzed via FISH using an OSCC tissue chip (n = 62). (E) Transwell migration and invasion assays using OSCC cells transfected with the miR-142-5p inhibitor or mimic. (F) Wound-healing assays were performed in OSCC cells transfected with the miR-142-5p inhibitor or mimic. (G) CCK-8 assays were performed in OSCC cells transfected with the miR-142-5p inhibitor or mimic. (H) Colony-formation assays were performed in OSCC cells transfected with the miR-142-5p inhibitor or mimic. (I) Apoptosis assays were performed in OSCC cells transfected with the miR-142-5p inhibitor or mimic. All data are presented as mean ± SEM of three independent experiments. Student's t test, *$p < 0.05$, **$p < 0.01$, ***$p < 0.001$. Representative images are shown. Scale bars, 20 μm.

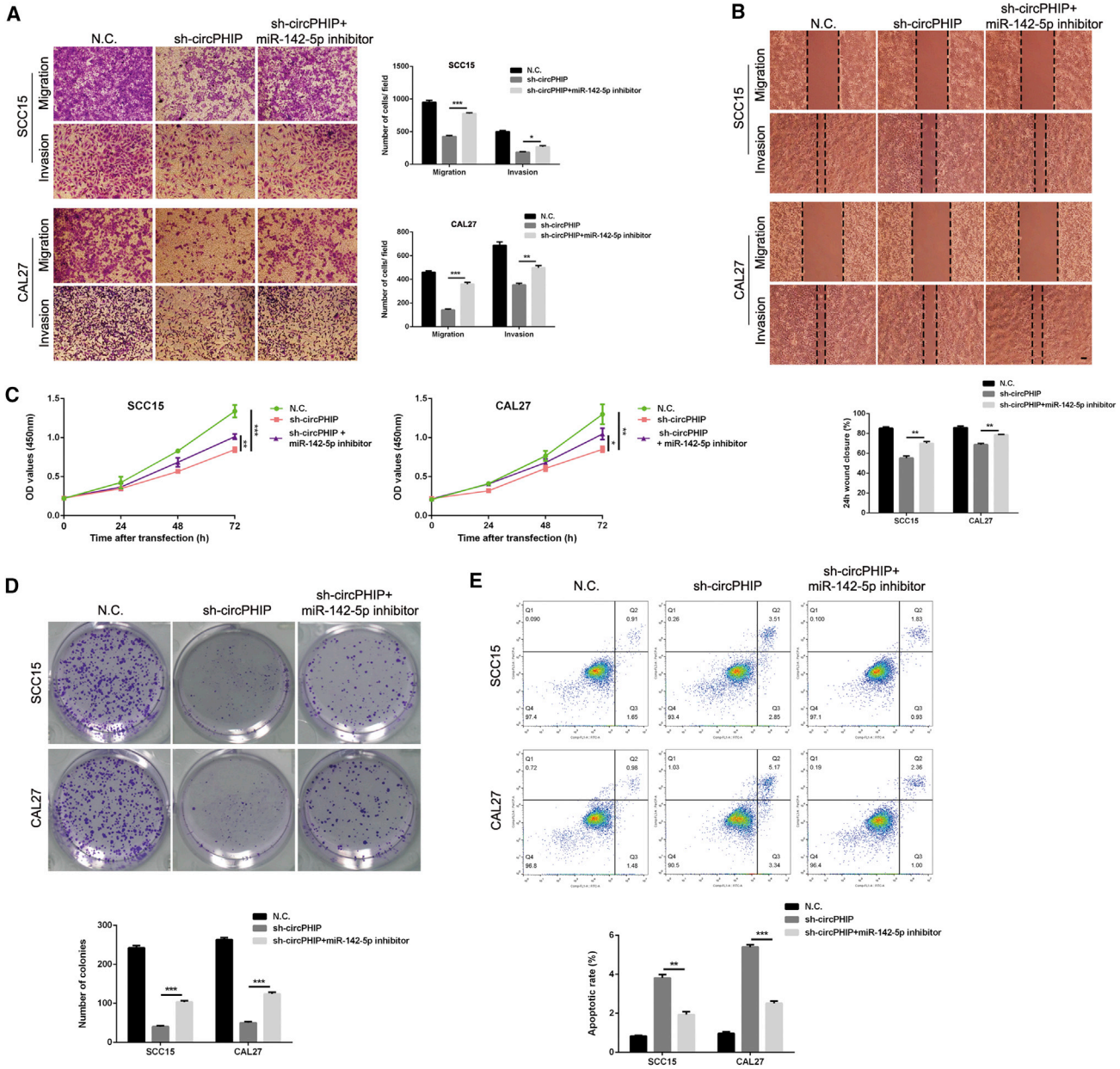

Figure 5. Depletion of miR-142-5p reverses sh-circPHIP-induced attenuation of OSCC cell migration, invasion, and proliferation

(A) Transwell migration and invasion assays with SCC15 and CAL27 cells stably transfected with the NC vector or sh-circPHIP, with or without the miR-142-5p inhibitor. (B) Wound-healing assays were performed in SCC15 and CAL27 cells stably transfected with NC or sh-circPHIP, with or without the miR-142-5p inhibitor. (C) CCK-8 assays were performed in SCC15 and CAL27 cells stably transfected with NC or sh-circPHIP, with or without the miR-142-5p inhibitor. (D) Colony-formation assays were performed in SCC15 and CAL27 cells stably transfected with NC or sh-circPHIP, with or without the miR-142-5p inhibitor. (E) Apoptosis assays were performed in SCC15 and CAL27 cells stably transfected with NC or sh-circPHIP, with or without the miR-142-5p inhibitor. All data are presented as mean ± SEM of three independent experiments. Student's t test, *$p < 0.05$, **$p < 0.01$, ***$p < 0.001$. Representative images are shown. Scale bars, 20 μm.

OSCC. Interestingly, circPHIP regulates PHIP expression to affect the malignant behavior of OSCC, as it is transcribed from the *PHIP* gene.

ACTN4 is located on human chromosome 19 and encodes an actin crosslinking protein.[43] ACTN4 overexpression in cancer cells stimulates the dynamic remodeling of the actin cytoskeleton, resulting in an increased metastatic potential.[44] ACTN4 is involved in the progression and metastasis of many cancer types, including breast, colorectal, and pancreatic cancers.[45–47]

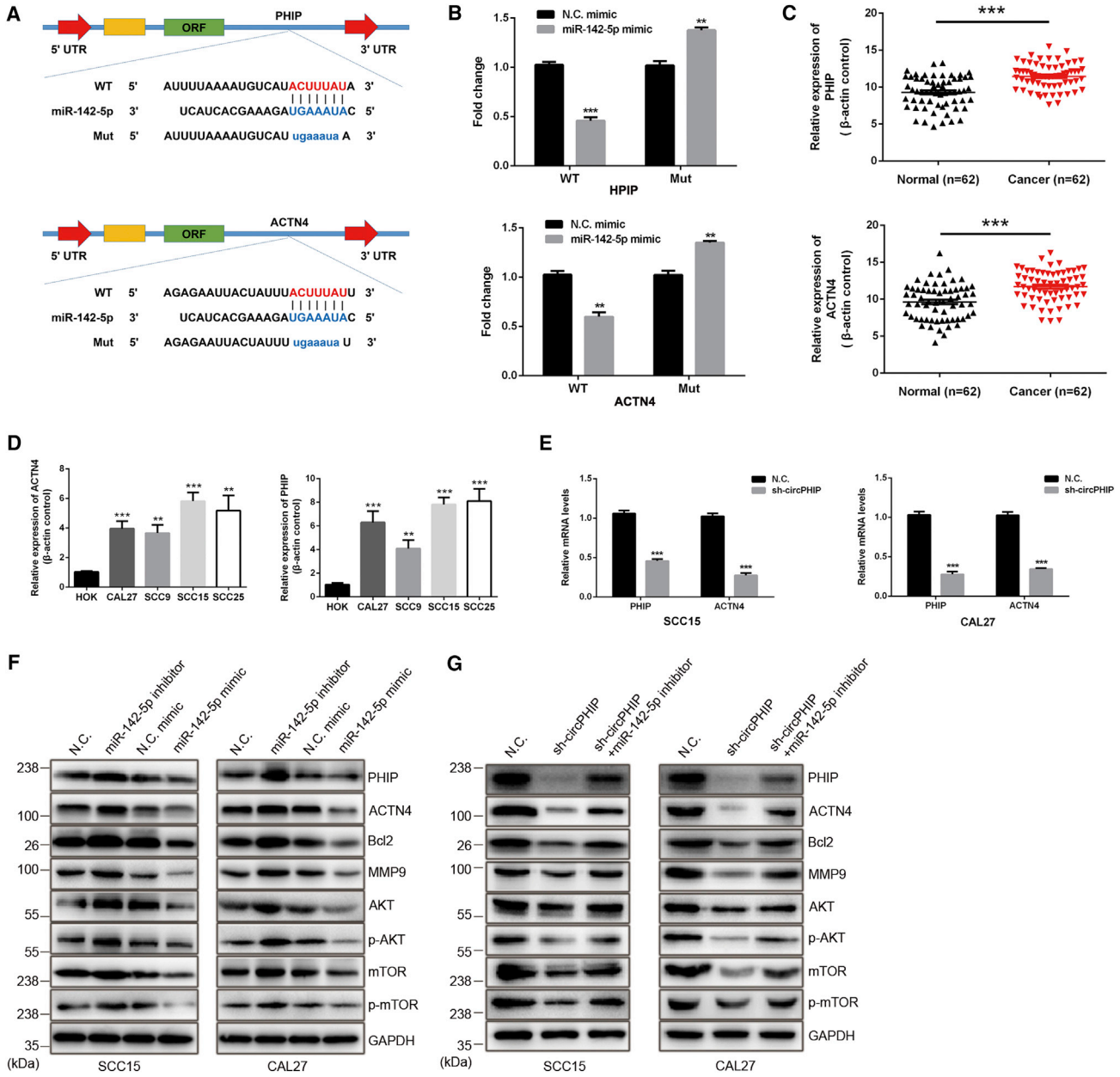

Figure 6. *PHIP* and *ACTN4* are direct targets of miR-142-5p

(A) Schematic of the complementary sequence between miR-142-5p and *PHIP* and *ACTN4*. Mut nucleotides in the *PHIP* and *ACTN4* 3′ UTRs are in lowercase. (B) HOKs were cotransfected with the miR-142-5p or NC mimics and luciferase reporter constructs containing WT or Mut of *PHIP* or *ACTN4* 3′ UTRs. The luciferase activities were detected. (C) qRT-PCR was used to detect *ACTN4* and *PHIP* expression in OSCC tissues. (D) qRT-PCR was used to compare *ACTN4* and *PHIP* expression in OSCC and healthy cell lines. (E) *PHIP* and *ACTN4* expression in SCC15 and CAL27 cells transfected with NC or sh-circPHIP was determined via qRT-PCR. Relative mRNA levels are shown. (F) OSCC cells were transfected with the miR-142-5p inhibitor or mimic and analyzed via western blotting. (G) SCC15 and CAL27 cells were transfected with sh-circPHIP, with or without the miR-142-5p inhibitor, and the indicated protein levels were detected via western blotting. All data are presented as mean ± SEM of three independent experiments. Student's t test, $^{**}p < 0.01$, $^{***}p < 0.001$. Representative images are shown.

The PI3K/AKT/mTOR signaling pathway plays important roles in tumor development and progression. Gain- or loss-of-function in the pathway due to the abnormal expression of its components can affect proliferation, apoptosis, and invasion in tumor cells.[48] Our research indicates that PHIP and ACTN4 could activate this signaling pathway, promoting p-AKT and p-mTOR and initiating a cascade of downstream signaling pathways that promote malignant behavior.

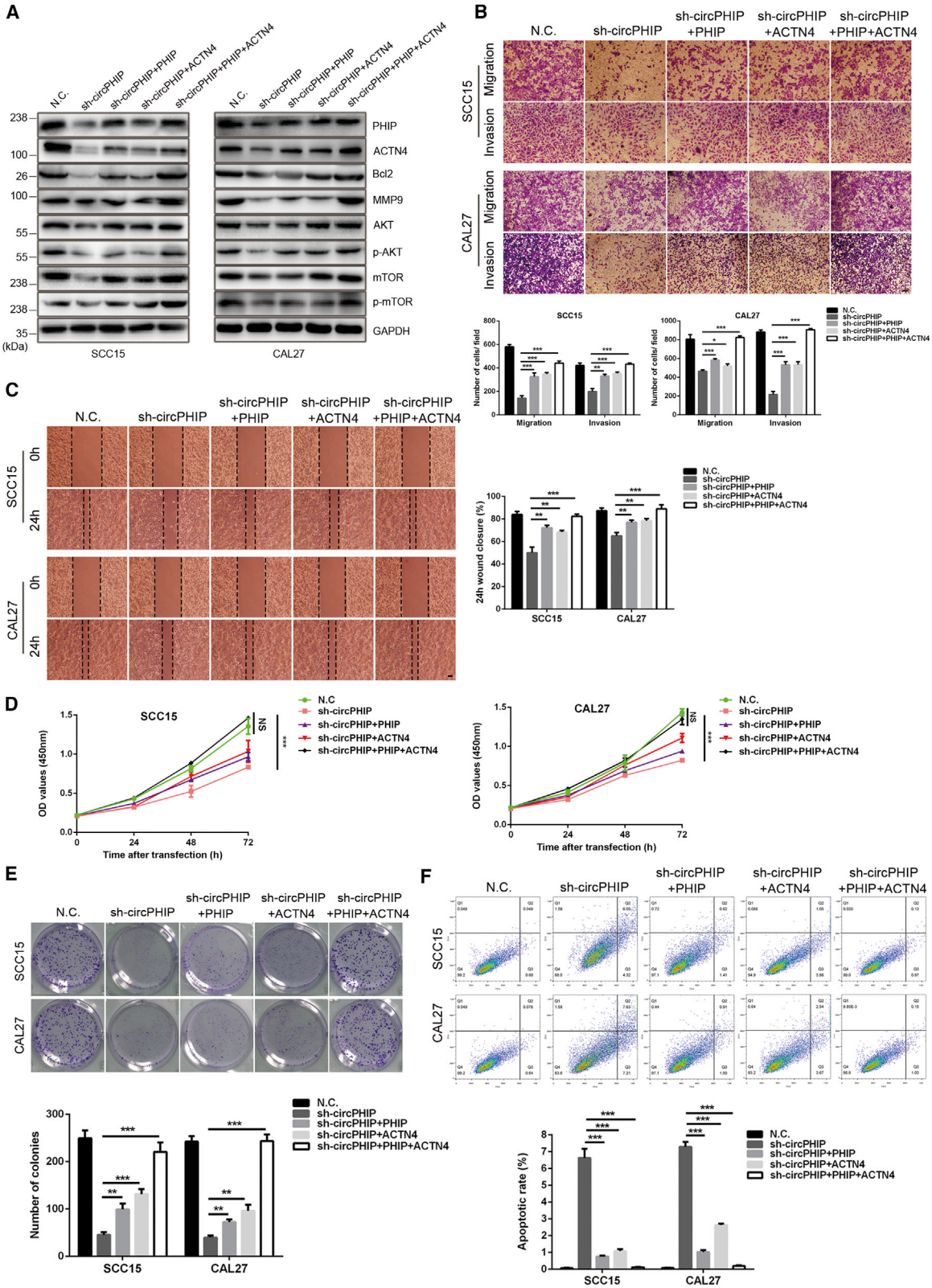

(legend on next page)

Multiple studies have shown that certain noncoding RNAs can be stably and repeatedly detected in body fluids, making them promising biomarkers or even therapeutic targets in certain diseases.[49,50] However, whether circPHIP can be stably detected in bodily fluids, such as peripheral blood or saliva, requires further study.

In summary, our research indicates that circPHIP is highly expressed in both OSCC tissues and cell lines and that *PHIP* and *ACTN4* act as oncogenes in OSCC development and progression. Moreover, overexpression of PHIP and ACTN4 can activate PI3K/AKT/mTOR signaling. Mechanistically, circPHIP promotes OSCC progression and metastasis by adsorbing miR-142-5p and increasing PHIP and ACTN4 expression. This circPHIP/miR-142-5p/PHIP-ACTN4 axis provides new strategies for targeted therapies for OSCC.

MATERIALS AND METHODS

Clinical samples and ethical approval

The study was approved by the Ethics Committee of the Peking University Health Science Center (IRB00001053-08043) and strictly adhered to the Code of Ethics of Peking University (protocol number 37923/2-3-2012). All patient tissue samples were obtained from the Stomatological Center of Peking University Shenzhen Hospital (Shenzhen, China) in accordance with the Declaration of Helsinki. All patients provided written consent. The histopathological grading of tumors was performed according to the 2018 World Health Organization classification criteria for head and neck cancer. Tissue samples were immediately frozen in liquid nitrogen and stored at −80°C.

RNA extraction and qRT-PCR

Total RNA was extracted from surgical specimens using TRIzol (Life Technologies, Carlsbad, CA, USA). RNA concentrations were evaluated using the Nanodrop ND-1000 spectrophotometer (Thermo Fisher Scientific, Waltham, MA, USA). Total RNA was isolated with the RNeasy Mini Kit (QIAGEN, Hilden, Germany). Samples were treated with 3 U/mg RNase R for 15 min at 37°C (Epicenter, Madison, WI, USA). Treated RNA (500 ng) was directly reverse transcribed using the PrimeScript RT Master Mix (Takara Bio, Kusatsu, Japan) with random or oligo (dT) primers. PCR was performed using the PCR Master Mix (2×) (Thermo Fisher Scientific). The $2^{-\Delta\Delta Ct}$ method was used to calculate the relative expression of the different genes, and glyceraldehyde 3-phosphate dehydrogenase (*GAPDH*) was used as an internal control.

Library construction, sequencing, and data analysis

Details on library construction, sequencing, and data analysis were described previously.[29] The strand-specific library was constructed using the VAHTS Total RNA-seq (H/M/R) Library Prep Kit (Illumina, San Diego, CA, USA), following the manufacturer's protocol. PCR amplification and sequencing using Illumina HiSeq 2500 was performed by Gene Denovo Biotechnology (Guangzhou, China). To quantify high-quality circRNAs, the back-spliced junction reads were scaled to reads per million of mapped reads, thereby eliminating the influence of different amounts of sequencing data on calculating circRNA expression levels. The calculated expression can be used to compare the differential expression of circRNAs among groups. To identify differentially expressed circRNAs across groups, the edgeR package (https://www.bioconductor.org/) was used. We identified circRNAs with a fold change ≥ 2 and a p value <0.05 as significant differentially expressed circRNAs.

Cell culture and treatment

Human OSCC cell lines (SCC9, SCC15, SCC25, and CAL27) were gifts from Wuhan University (Wuhan, China). HOKs were obtained from the cell bank of the Chinese Academy of Sciences (Shanghai, China). All cell lines were mycoplasma free and were cultured in Dulbecco's modified Eagle's medium (DMEM; Gibco, Grand Island, NY, USA), supplemented with 10% fetal bovine serum (Gibco), 100 U/mL penicillin, and 100 U/mL streptomycin (Invitrogen, Carlsbad, CA, USA) at 37°C in a humidified atmosphere with 5% CO_2.

shRNA, vector construction, and stable transfection

miRNA inhibitors and mimics were purchased from RiboBio (Guangzhou, China). Lipofectamine 3000 (Invitrogen) was used for transfections. A lentiviral vector (pHBLV-CMV-crRNA-EF1-GFP-T2Apuro) was constructed by HanBio (Shanghai, China). After 48 h of lentiviral infection, a stable cell line was selected using puromycin (8 μg/mL for SCC15 cells; 10 μg/mL for CAL27 cells; RiboBio).

FISH

The Ribo FISH Kit (RiboBio, Guangzhou, China) was used for FISH experiments. Probes and experimental reagents were designed and synthesized by RiboBio. The slides were placed at the bottom of a 24-well plate and seeded with 6×10^4 cells per well. Cells were cultured to 60%–70% confluency prior to experiments. Prechilled permeate and 4% paraformaldehyde were used for cell permeation and fixation, respectively. Fixed cells were incubated with a circPHIP FISH Probe Mix stock solution or an internal reference FISH Probe Mix stock for probe detection, and nuclei were stained with 4′,6-diamidino-2-phenylindole (DAPI). After mounting, images were acquired under a fluorescence microscope (Eclipse E600; Nikon, Tokyo, Japan). The expression level of miR-142-5p in tissues was assessed via FISH using an miR-142-5p-specific probe on tissue arrays containing 62 samples (Alenabio,

Figure 7. *PHIP* and *ACTN4* function as driver genes in OSCC cells

(A) Overexpression of PHIP and ACTN4 in SCC15 and CAL27 cells with stable depletion of circPHIP, and the levels of indicated proteins were determined via western blotting. (B) Transwell migration and invasion assays were performed in SCC15 and CAL27 cells with stable depletion of circPHIP and PHIP or ACTN4 overexpression. (C) Wound-healing assays were performed in SCC15 and CAL27 cells with stable depletion of circPHIP and PHIP or ACTN4 overexpression. (D) CCK-8 assays were performed in SCC15 and CAL27 cells with stable depletion of circPHIP and PHIP or ACTN4 overexpression. (E) Colony-formation assays were performed in SCC15 and CAL27 cells with stable depletion of circPHIP and PHIP/ACTN4 overexpression. (F) Apoptosis assays were performed in SCC15 and CAL27 cells stably depleting circPHIP and PHIP or ACTN4 overexpression. All data are presented as mean ± SEM of three independent experiments. Student's t test, *p < 0.05, **p < 0.01, ***p < 0.001. Representative images are shown. Scale bars, 20 μm.

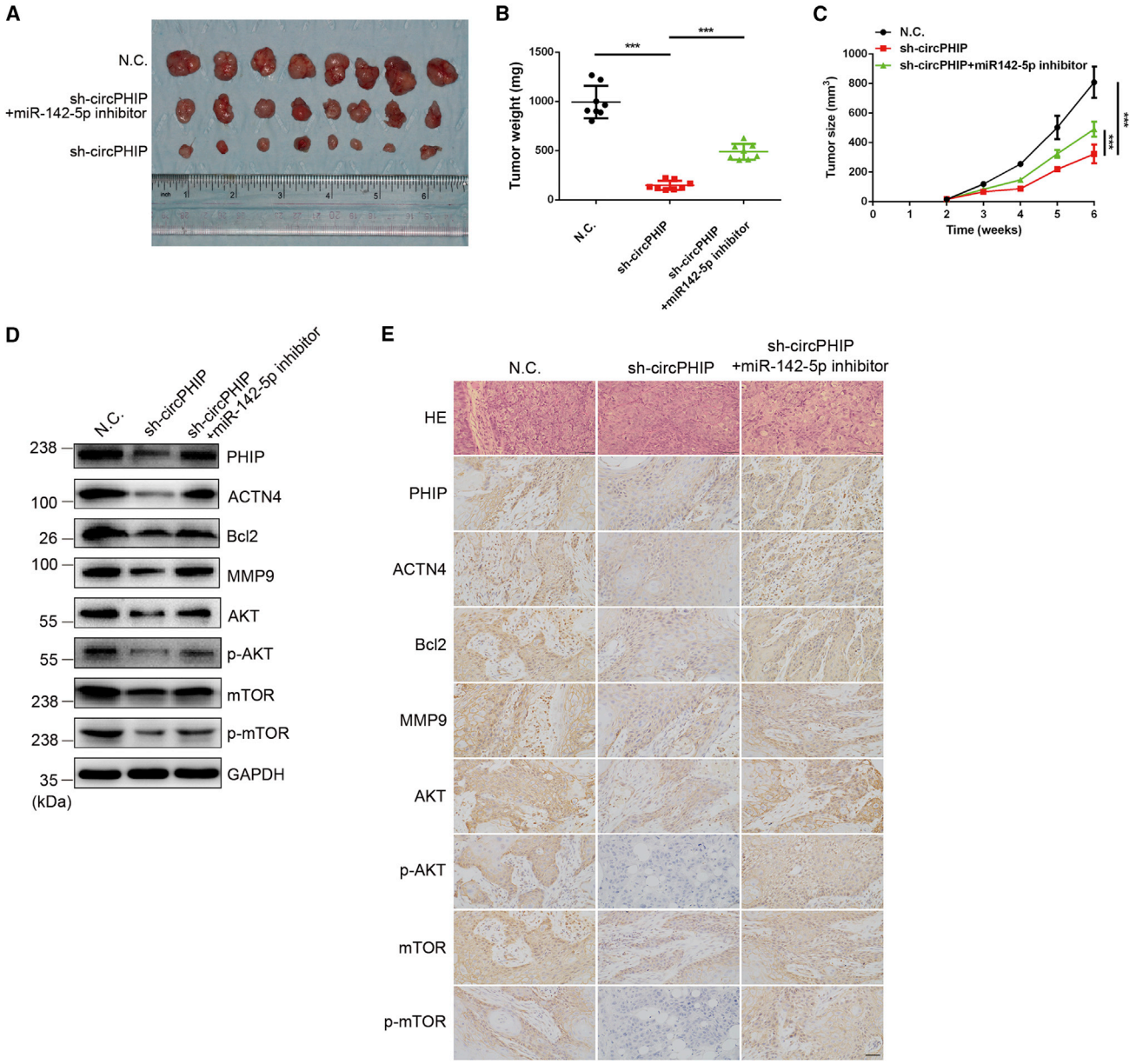

Figure 8. circPHIP functions as an miR-142-5p sponge to promote tumorigenesis *in vivo*

(A) Nude mice were subcutaneously injected with 5×10^6 SCC15 cells or cells stably expressing sh-circPHIP or with the miR-142-5p inhibitor (n = 8 per group). (B) Tumor weights from euthanized mice. (C) Weekly measurements of tumor volumes were recorded every 6 days starting the day mice were injected with SCC15 cells stably expressing sh-circPHIP. (D) The indicated protein levels in tumors from the different groups were analyzed via western blotting. (E) H&E and IHC staining were performed using OSCC xenografts from the different groups. All data are presented as mean ± SEM. Student's t test, ***$p < 0.001$. Representative images are shown. Scale bars, 100 μm.

China) and evaluated using the quantitative scanning method under Aperio ImageScope V11 from Leica (Wetzlar, Germany). The positivity value represents the expression level of miR-142-5p.

RIP

RIP experiments were performed using the Magna RIP RNA-Binding Protein Immunoprecipitation Kit (Millipore, Billerica, MA, USA). An AGO2-containing plasmid was transfected into HOKs. Cells were detached from plates using trypsin and collected via centrifugation (12,000 × *g* at 4°C for 10 min), and 1×10^7 cells were lysed in 100 μL RIP lysis buffer containing RNase and protease inhibitors. Beads were coated with antibodies against AGO2 (Millipore) or rabbit immunoglobulin G (IgG) and incubated with lysates overnight at 4°C. Immunoprecipitated RNA was then treated with proteinase K

(RiboBio) and an RNeasy MinElute Cleanup Kit (QIAGEN). The circPHIP content was analyzed using qRT-PCR.

RNA pulldown assays

SCC15 and CAL27 cells were collected, lysed, and sonicated. A circPHIP probe, designed and synthesized by RiboBio, was incubated with C-1 magnetic beads (Life Technologies) at 25°C for 2 h and then with cell lysates overnight at 4°C. RNA complexes bound to the C-1 magnetic beads were eluted, purified with the RNeasy Mini Kit (QIAGEN), and analyzed via qRT-PCR.

Luciferase reporter assays

Reporter plasmids (pGL3-Firefly luciferase-*Renilla* luciferase, containing circPHIP, *PHIP*, or *ACTN4* 3′ UTR or corresponding Muts) were designed by HanBio. HOKs were cotransfected with a reporter plasmid and either the miR-142-5p mimic or NC mimic (RiboBio). Firefly luciferase activity was normalized to *Renilla* luciferase activity.

Colony-formation assays

Transfected cells (1×10^3) were uniformly distributed in 6-well plates and cultured for 2 weeks. The cells were then washed with phosphate-buffered saline, fixed with 4% paraformaldehyde, stained with 0.5% crystal violet, and imaged.

Western blotting analysis

Cell and tissue specimens were prepared at 4°C in radioimmunoprecipitation assay buffer (RIPA buffer) containing a protease inhibitor (MA0151; Dalian Meilun Biotechnology, Dalian, China). Primary antibodies against PHIP (1:2,000; ab86244), Bcl-2 (1:2,000; ab32124), MMP9 (1:2,000; ab38898), and GAPDH (1:2,000; ab8245) were purchased from Abcam (Cambridge, UK). Primary antibodies against AKT serine/threonine kinase 1 (AKT1; 1:1,000; #4691), p-AKT (Ser473) (1:2,000; #4060), mTOR (1:1,000; #2983), p-mTOR (Ser2448) (1:1,000; #5536), and ACTN4 (1:1,000; #15145) were purchased from Cell Signaling Technology (Danvers, MA, USA). Horseradish peroxidase-conjugated secondary antibodies, including goat anti-rabbit (1:1,000; A0208) and goat anti-mouse (1:1,000; A0216) antibodies, were purchased from Beyotime Biotechnology (Shanghai, China). Electrochemiluminescence visualization of proteins was performed using a Millipore chemical developer (Millipore Sigma, Burlington, MA, USA).

Tumor xenograft formation and staining

The Animal Experimentation Ethics Committee of Shenzhen Peking University, Hong Kong University of Science and Technology Medical Center, approved our study and ensured that all experiments conformed to all relevant regulatory standards. Differently transfected SCC15 cells (1×10^7 cells/100 μL) were subcutaneously injected into 4-week-old BALB/c athymic nude mice (Hunan Jingke Experimental Animal, Hunan, China). Tumor volume (V) was measured weekly and calculated using the equation $V = (a \times b^2)/2$, where a and b are the length and width of the tumor, respectively. After 6 weeks, the mice were euthanized, and tumors were dissected for hematoxylin and eosin (H&E) and IHC staining.

Additional *in vitro* experiments

Transwell migration and invasion assays, qRT-PCR analysis, CCK-8 assays, wound-healing assays, EdU incorporation assays, apoptosis assays, flow cytometry, H&E staining, and IHC staining were performed as previously described.[51]

Statistical analyses

Statistical analyses were performed using SPSS 20 software (IBM, Armonk, NY, USA). Data represent the mean ± standard error of the mean (SEM) of three independent experiments or are representative of three independent experiments with similar results (*$p < 0.05$ versus the control sample or as indicated, using Student's t test)

Data accessibility

The datasets used and/or analyzed during the current study are available from the corresponding author on reasonable request.

SUPPLEMENTAL INFORMATION

Supplemental Information can be found online at https://doi.org/10.1016/j.omtn.2020.10.038.

ACKNOWLEDGMENTS

This study was supported by the National Natural Science Foundation of China (grant number 81902758); National Natural Science Foundation of Guangdong Province (2019A1515011911); Basic Research Program of the Shenzhen Innovation Council of China (grant numbers JCYJ20180228175511141, JCYJ20170306161518559, and SZBC2017023); and Sanming Project of Medicine in Shenzhen (SZSM 201512036, Oral and Maxillofacial Surgery Team, Professor Yu Guangyan, Peking University Hospital of Stomatology), and Shenzhen Fund for Guangdong Provincial High-level Clinical Key Specialties (number SZGSP008) to the Department of Oral and Maxillofacial Surgery, Peking University Shenzhen Hospital, Shenzhen, Guangdong, China.

AUTHOR CONTRIBUTIONS

Conceptualization, W.S., Y.S., and H.Y.; Data Curation, W.S.; Formal Analysis, W.S.; Funding Acquisition, Y.S., Y.W., X.H., and H.Y.; Investigation, W.S., Y.S., Y.W., F.W., X.H., Y.C., and Y.L.; Methodology, W.S.; Project Administration, Y.S. and H.Y.; Supervision, Y.S. and H.Y.; Writing – Original Draft, W.S.; Writing – Review & Editing, Y.S. and H.Y. All authors have read and approved the final manuscript.

DECLARATION OF INTERESTS

The funding organizations had no role in the design of the study, analysis, and interpretation of the data or in writing the manuscript. The authors declare no competing interests.

REFERENCES

1. Warnakulasuriya, S. (2009). Global epidemiology of oral and oropharyngeal cancer. Oral Oncol. *45*, 309–316.

2. Jemal, A., Siegel, R., Ward, E., Hao, Y., Xu, J., and Thun, M.J. (2009). Cancer statistics, 2009. CA Cancer J. Clin. *59*, 225–249.

3. Omura, K. (2014). Current status of oral cancer treatment strategies: surgical treatments for oral squamous cell carcinoma. Int. J. Clin. Oncol. *19*, 423–430.
4. Trotta, B.M., Pease, C.S., Rasamny, J.J., Raghavan, P., and Mukherjee, S. (2011). Oral cavity and oropharyngeal squamous cell cancer: key imaging findings for staging and treatment planning. Radiographics *31*, 339–354.
5. Dibble, E.H., Alvarez, A.C., Truong, M.T., Mercier, G., Cook, E.F., and Subramaniam, R.M. (2012). 18F-FDG metabolic tumor volume and total glycolytic activity of oral cavity and oropharyngeal squamous cell cancer: adding value to clinical staging. J. Nucl. Med. *53*, 709–715.
6. Jeck, W.R., Sorrentino, J.A., Wang, K., Slevin, M.K., Burd, C.E., Liu, J., Marzluff, W.F., and Sharpless, N.E. (2013). Circular RNAs are abundant, conserved, and associated with ALU repeats. RNA *19*, 141–157.
7. Jeck, W.R., and Sharpless, N.E. (2014). Detecting and characterizing circular RNAs. Nat. Biotechnol. *32*, 453–461.
8. Guo, J.U., Agarwal, V., Guo, H., and Bartel, D.P. (2014). Expanded identification and characterization of mammalian circular RNAs. Genome Biol. *15*, 409.
9. Liu, G., Huang, K., Jie, Z., Wu, Y., Chen, J., Chen, Z., Fang, X., and Shen, S. (2018). CircFAT1 sponges miR-375 to promote the expression of Yes-associated protein 1 in osteosarcoma cells. Mol. Cancer *17*, 170.
10. Barbagallo, D., Caponnetto, A., Brex, D., Mirabella, F., Barbagallo, C., Lauretta, G., Morrone, A., Certo, F., Broggi, G., Caltabiano, R., et al. (2019). CircSMARCA5 regulates VEGFA mRNA splicing and angiogenesis in glioblastoma multiforme through the binding of SRSF1. Cancers (Basel) *11*, E194.
11. Legnini, I., Di Timoteo, G., Rossi, F., Morlando, M., Briganti, F., Sthandier, O., Fatica, A., Santini, T., Andronache, A., Wade, M., et al. (2017). Circ-ZNF609 is a circular RNA that can be translated and functions in myogenesis. Mol. Cell *66*, 22–37.e9.
12. Pamudurti, N.R., Bartok, O., Jens, M., Ashwal-Fluss, R., Stottmeister, C., Ruhe, L., Hanan, M., Wyler, E., Perez-Hernandez, D., Ramberger, E., et al. (2017). Translation of CircRNAs. Mol. Cell *66*, 9–21.e7.
13. Liu, C.X., Li, X., Nan, F., Jiang, S., Gao, X., Guo, S.K., Xue, W., Cui, Y., Dong, K., Ding, H., et al. (2019). Structure and degradation of circular RNAs regulate PKR activation in innate immunity. Cell *177*, 865–880.e21.
14. Chen, S., Huang, V., Xu, X., Livingstone, J., Soares, F., Jeon, J., Zeng, Y., Hua, J.T., Petricca, J., Guo, H., et al. (2019). Widespread and functional RNA circularization in localized prostate cancer. Cell *176*, 831–843.2e22.
15. Zhang, M., Zhao, K., Xu, X., Yang, Y., Yan, S., Wei, P., Liu, H., Xu, J., Xiao, F., Zhou, H., et al. (2018). A peptide encoded by circular form of LINC-PINT suppresses oncogenic transcriptional elongation in glioblastoma. Nat. Commun. *9*, 4475.
16. Vo, J.N., Cieslik, M., Zhang, Y., Shukla, S., Xiao, L., Zhang, Y., Wu, Y.M., Dhanasekaran, S.M., Engelke, C.G., Cao, X., et al. (2019). The landscape of circular RNA in cancer. Cell *176*, 869–881.e13.
17. Denli, A.M., Tops, B.B., Plasterk, R.H., Ketting, R.F., and Hannon, G.J. (2004). Processing of primary microRNAs by the Microprocessor complex. Nature *432*, 231–235.
18. Gebert, L.F.R., and MacRae, I.J. (2019). Regulation of microRNA function in animals. Nat. Rev. Mol. Cell Biol. *20*, 21–37.
19. Rupaimoole, R., and Slack, F.J. (2017). MicroRNA therapeutics: towards a new era for the management of cancer and other diseases. Nat. Rev. Drug Discov. *16*, 203–222.
20. Bracken, C.P., Scott, H.S., and Goodall, G.J. (2016). A network-biology perspective of microRNA function and dysfunction in cancer. Nat. Rev. Genet. *17*, 719–732.
21. Rupaimoole, R., Calin, G.A., Lopez-Berestein, G., and Sood, A.K. (2016). miRNA deregulation in cancer cells and the tumor microenvironment. Cancer Discov. *6*, 235–246.
22. Kristensen, L.S., Andersen, M.S., Stagsted, L.V.W., Ebbesen, K.K., Hansen, T.B., and Kjems, J. (2019). The biogenesis, biology and characterization of circular RNAs. Nat. Rev. Genet. *20*, 675–691.
23. Memczak, S., Jens, M., Elefsinioti, A., Torti, F., Krueger, J., Rybak, A., Maier, L., Mackowiak, S.D., Gregersen, L.H., Munschauer, M., et al. (2013). Circular RNAs are a large class of animal RNAs with regulatory potency. Nature *495*, 333–338.
24. Taulli, R., Loretelli, C., and Pandolfi, P.P. (2013). From pseudo-ceRNAs to circ-ceRNAs: a tale of cross-talk and competition. Nat. Struct. Mol. Biol. *20*, 541–543.
25. Hansen, T.B., Jensen, T.I., Clausen, B.H., Bramsen, J.B., Finsen, B., Damgaard, C.K., and Kjems, J. (2013). Natural RNA circles function as efficient microRNA sponges. Nature *495*, 384–388.
26. Tay, Y., Rinn, J., and Pandolfi, P.P. (2014). The multilayered complexity of ceRNA crosstalk and competition. Nature *505*, 344–352.
27. Rivera, C. (2015). Essentials of oral cancer. Int. J. Clin. Exp. Pathol. *8*, 11884–11894.
28. Wang, Y.F., Li, B.W., Sun, S., Li, X., Su, W., Wang, Z.H., Wang, F., Zhang, W., and Yang, H.Y. (2018). Circular RNA expression in oral squamous cell carcinoma. Front. Oncol. *8*, 398.
29. Maddika, S., Ande, S.R., Panigrahi, S., Paranjothy, T., Weglarczyk, K., Zuse, A., Eshraghi, M., Manda, K.D., Wiechec, E., and Los, M. (2007). Cell survival, cell death and cell cycle pathways are interconnected: implications for cancer therapy. Drug Resist. Updat. *10*, 13–29.
30. Jacob, A., and Prekeris, R. (2015). The regulation of MMP targeting to invadopodia during cancer metastasis. Front. Cell Dev. Biol. *3*, 4.
31. Alzahrani, A.S. (2019). PI3K/Akt/mTOR inhibitors in cancer: At the bench and bedside. Semin. Cancer Biol. *59*, 125–132.
32. Hanniford, D., Ulloa-Morales, A., Karz, A., Berzoti-Coelho, M.G., Moubarak, R.S., Sánchez-Sendra, B., Kloetgen, A., Davalos, V., Imig, J., Wu, P., et al. (2020). Epigenetic silencing of CDR1as drives IGF2BP3-mediated melanoma invasion and metastasis. Cancer Cell *37*, 55–70.e15.
33. Wu, P., Mo, Y., Peng, M., Tang, T., Zhong, Y., Deng, X., Xiong, F., Guo, C., Wu, X., Li, Y., et al. (2020). Emerging role of tumor-related functional peptides encoded by lncRNA and circRNA. Mol. Cancer *19*, 22.
34. Bartel, D.P. (2009). MicroRNAs: target recognition and regulatory functions. Cell *136*, 215–233.
35. Salmena, L., Poliseno, L., Tay, Y., Kats, L., and Pandolfi, P.P. (2011). A ceRNA hypothesis: the Rosetta Stone of a hidden RNA language? Cell *146*, 353–358.
36. Abdollahzadeh, R., Daraei, A., Mansoori, Y., Sepahvand, M., Amoli, M.M., and Tavakkoly-Bazzaz, J. (2019). Competing endogenous RNA (ceRNA) cross talk and language in ceRNA regulatory networks: A new look at hallmarks of breast cancer. J. Cell. Physiol. *234*, 10080–10100.
37. Qu, L., Ding, J., Chen, C., Wu, Z.J., Liu, B., Gao, Y., Chen, W., Liu, F., Sun, W., Li, X.F., et al. (2016). Exosome-transmitted lncARSR promotes sunitinib resistance in renal cancer by acting as a competing endogenous RNA. Cancer Cell *29*, 653–668.
38. Podcheko, A., Northcott, P., Bikopoulos, G., Lee, A., Bommareddi, S.R., Kushner, J.A., Farhang-Fallah, J., and Rozakis-Adcock, M. (2007). Identification of a WD40 repeat-containing isoform of PHIP as a novel regulator of beta-cell growth and survival. Mol. Cell. Biol. *27*, 6484–6496.
39. Haqq, C., Nosrati, M., Sudilovsky, D., Crothers, J., Khodabakhsh, D., Pulliam, B.L., Federman, S., Miller, J.R., 3rd, Allen, R.E., Singer, M.I., et al. (2005). The gene expression signatures of melanoma progression. Proc. Natl. Acad. Sci. USA *102*, 6092–6097.
40. Bezrookove, V., Nosrati, M., Miller, J.R., 3rd, De Semir, D., Dar, A.A., Vosoughi, E., Vaquero, E., Sucker, A., Lazar, A.J., Gershenwald, J.E., et al. (2018). Role of elevated PHIP copy number as a prognostic and progression marker for cutaneous melanoma. Clin. Cancer Res. *24*, 4119–4125.
41. de Semir, D., Bezrookove, V., Nosrati, M., Dar, A.A., Wu, C., Shen, J., Rieken, C., Venkatasubramanian, M., Miller, J.R., 3rd, Desprez, P.Y., et al. (2018). PHIP as a therapeutic target for driver-negative subtypes of melanoma, breast, and lung cancer. Proc. Natl. Acad. Sci. USA *115*, E5766–E5775.
42. De Semir, D., Nosrati, M., Bezrookove, V., Dar, A.A., Federman, S., Bienvenu, G., Venna, S., Rangel, J., Climent, J., Meyer Tamgüney, T.M., et al. (2012). Pleckstrin homology domain-interacting protein (PHIP) as a marker and mediator of melanoma metastasis. Proc. Natl. Acad. Sci. USA *109*, 7067–7072.
43. Otey, C.A., and Carpen, O. (2004). Alpha-actinin revisited: a fresh look at an old player. Cell Motil. Cytoskeleton *58*, 104–111.
44. Honda, K., Yamada, T., Endo, R., Ino, Y., Gotoh, M., Tsuda, H., Yamada, Y., Chiba, H., and Hirohashi, S. (1998). Actinin-4, a novel actin-bundling protein associated with cell motility and cancer invasion. J. Cell Biol. *140*, 1383–1393.
45. Khurana, S., Chakraborty, S., Cheng, X., Su, Y.T., and Kao, H.Y. (2011). The actin-binding protein, actinin alpha 4 (ACTN4), is a nuclear receptor coactivator that promotes proliferation of MCF-7 breast cancer cells. J. Biol. Chem. *286*, 1850–1859.

46. Honda, K., Yamada, T., Hayashida, Y., Idogawa, M., Sato, S., Hasegawa, F., Ino, Y., Ono, M., and Hirohashi, S. (2005). Actinin-4 increases cell motility and promotes lymph node metastasis of colorectal cancer. Gastroenterology *128*, 51–62.

47. Kikuchi, S., Honda, K., Tsuda, H., Hiraoka, N., Imoto, I., Kosuge, T., Umaki, T., Onozato, K., Shitashige, M., Yamaguchi, U., et al. (2008). Expression and gene amplification of actinin-4 in invasive ductal carcinoma of the pancreas. Clin. Cancer Res. *14*, 5348–5356.

48. Shaw, R.J., and Cantley, L.C. (2006). Ras, PI(3)K and mTOR signalling controls tumour cell growth. Nature *441*, 424–430.

49. Xing, Z., Lin, A., Li, C., Liang, K., Wang, S., Liu, Y., Park, P.K., Qin, L., Wei, Y., Hawke, D.H., et al. (2014). lncRNA directs cooperative epigenetic regulation downstream of chemokine signals. Cell *159*, 1110–1125.

50. Sun, Y.M., Wang, W.T., Zeng, Z.C., Chen, T.Q., Han, C., Pan, Q., Huang, W., Fang, K., Sun, L.Y., Zhou, Y.F., et al. (2019). circMYBL2, a circRNA from MYBL2, regulates FLT3 translation by recruiting PTBP1 to promote FLT3-ITD AML progression. Blood *134*, 1533–1546.

51. Su, W., Tang, J., Wang, Y., Sun, S., Shen, Y., and Yang, H. (2019). Long non-coding RNA highly up-regulated in liver cancer promotes epithelial-to-mesenchymal transition process in oral squamous cell carcinoma. J. Cell. Mol. Med. *23*, 2645–2655.

OMTN, Volume *23*

Supplemental Information

circPHIP promotes oral squamous cell carcinoma progression by sponging miR-142-5p and regulating PHIP and ACTN4 expression

Wen Su, Yuehong Shen, Yufan Wang, Feng Wang, Xia Hong, Yuling Chen, Yuntao Lin, and Hongyu Yang

Supplementary Figure 1

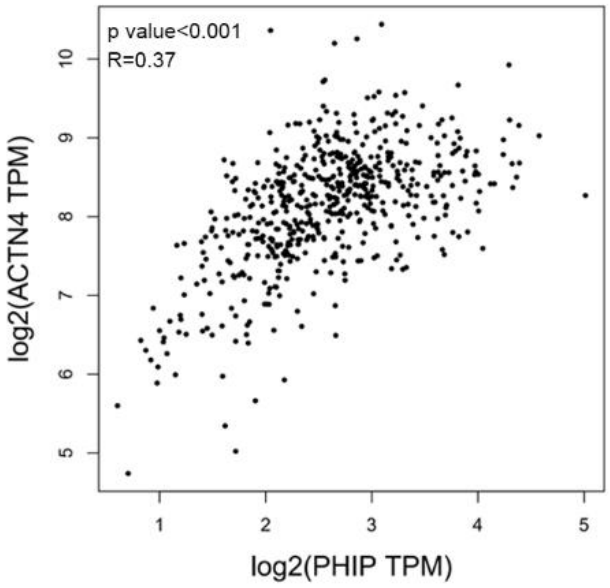

Supplementary Figure 1 Bioinformatics analysis of the correlation between PHIP and ACTN4 expression in head and neck tumors.

Supplementary Figure 2

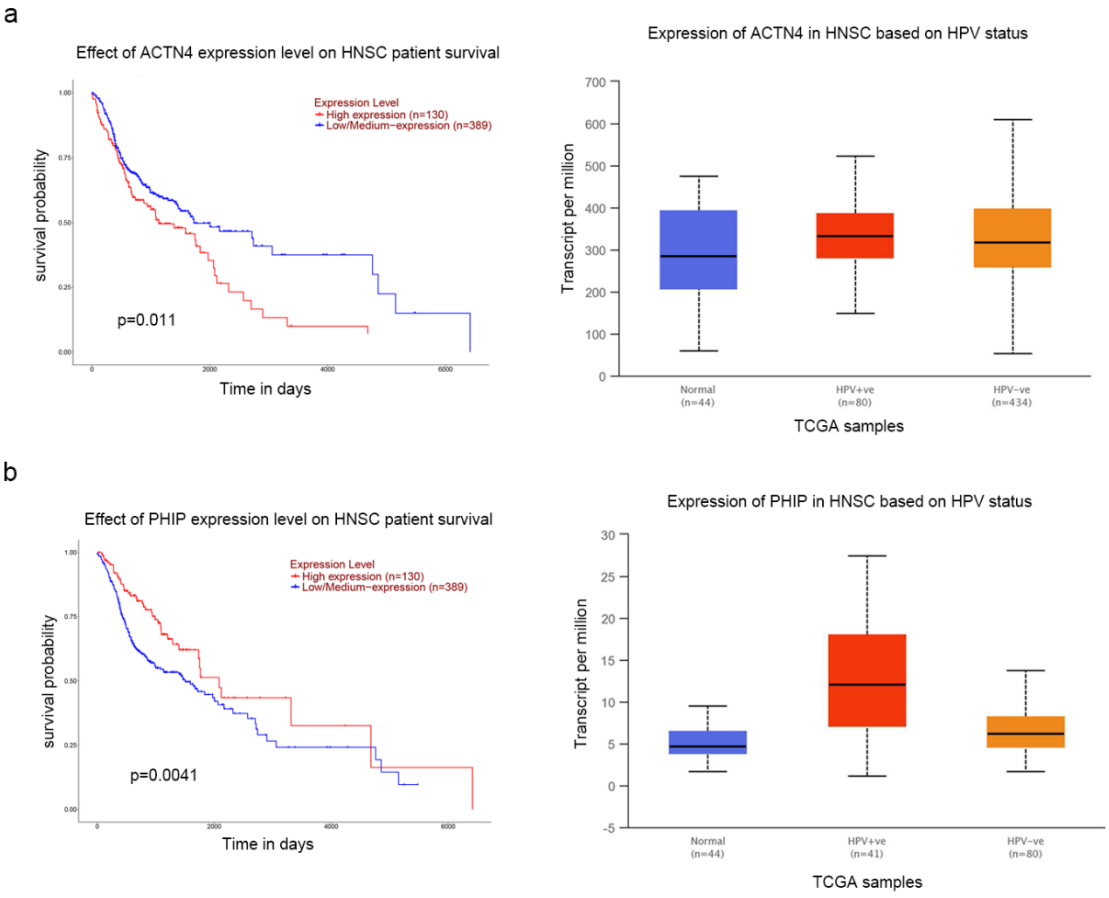

Supplementary Figure 2 a, b TCGA database analysis of the relationship between ACTN4 (a) or PHIP (b) expression and patient prognosis and HPV infection.

Supplementary Table 1 Correlation between clinicopathological features of patients with OSCC and circPHIP expression.

Parameter	No. of patients	Mean ± SEM	P value
Gender			
Male	38	11.38 ± 0.3444	0.8716
Female	24	11.30 ± 0.3132	
Age (yr)			
<60	25	11.66 ± 0.3292	0.3008
≥60	37	11.14 ± 0.3379	
Tumor size (cm)			
<5	52	11.35 ± 0.2633	0.9881
≥5	10	11.34 ± 0.6427	
Differentiation grade			
Well-moderate	40	11.60 ± 0.3184	0.1657
Poor-undifferentiated	22	10.89 ± 0.3476	
Lymph node status			
Negative	29	10.73 ± 0.3649	0.0149*
Positive	33	11.89 ± 0.2951	
TNM stage			
I-II	36	10.74 ± 0.3108	0.0023**
III-IV	26	12.19 ± 0.3218	
HPV stage			
Negative	48	10.98 ± 0.2669	0.0037**
Positive	14	12.62 ± 0.4139	